6740 *Inorg. Chem.* **2010**, *49*, 6740–6747
DOI: 10.1021/ic100845f

Inorganic Chemistry
Article

Single-Component Molecular Conductor [Cu(tmdt)$_2$] Containing an Antiferromagnetic Heisenberg Chain

Biao Zhou,[†] Hiroyuki Yajima,[†] Akiko Kobayashi,*[,†] Yoshinori Okano,[‡] Hisashi Tanaka,[§] Tetsuya Kumashiro,[∥] Eiji Nishibori,[∥] Hiroshi Sawa,[∥] and Hayao Kobayashi*[,†]

[†]*Department of Chemistry, College of Humanities and Sciences, Nihon University, Sakurajosui 3-25-40, Setagaya-Ku, Tokyo 156-8550, Japan,* [‡]*Institute for Molecular Science, Okazaki 444-8585, Japan,* [§]*Nanosystem Research Institute (NRI), AIST, Umezono, Tsukuba 305-8565, Japan, and* [∥]*Department of Applied Physics, Nagoya University, Nagoya 464-8603, Japan*

Received April 28, 2010

Traditional molecular conductors are composed of more than two chemical species and are characterized by low-dimensional electronic band structures. By contrast, the single-component molecular metals [M(tmdt)$_2$] (M = Ni, Pt, Au; tmdt = trimethylenetetrathiafulvalenedithiolate) possess three-dimensional electronic structures that can be widely tuned by exchanging the central transition metal atom (M). In this study, the Cu atom was used to realize a new magnetic single-component molecular conductor exhibiting strong $\pi-$d interactions. The crystal structure of [Cu(tmdt)$_2$] was found to be essentially the same as those of the Ni, Pt, or Au-based systems with metallic states down to low temperature, but different from the structure of [Cu(dmdt)$_2$] (dmdt = dimethyltetrathiafulvalenedithiolate) with its tetrahedrally coordinated dmdt ligands. A compressed pellet of microcrystals exhibited fairly high room-temperature conductivity ($\sigma_{RT} \sim 7$ S·cm^{-1}), which increased almost linearly with pressure, reaching 110 S·cm^{-1} at 15 kbar. This strongly suggests that the single crystal of [Cu(tmdt)$_2$] is metallic at high pressure. Magnetic susceptibility measurements indicated one-dimensional Heisenberg behavior with $|J| = 117$ cm^{-1} and an antiferromagnetic transition at 13 K. Density functional theory molecular orbital calculations revealed that the α-spin orbital of pdσ(-) is distributed at the central part of the complex (CuS_4), and α- and β-sym-Lπ orbitals have almost the same energies and their spins are distributed mainly in the pdσ(-) orbital. This is in contrast to the first single-component molecular metal [Ni(tmdt)$_2$], which has stable metal bands formed from an almost degenerated sym-Lπ orbital (the highest occupied molecular orbital) and asym-Lπ(d) orbital (the lowest unoccupied molecular orbital). These results suggest that the α-pdσ(-) state of [Cu(tmdt)$_2$] exists just around the Fermi energy of the *virtual* metal band formed from the asym-Lπ(d) and sym-Lπ states. Thus, as expected, [Cu(tmdt)$_2$] is a non-trivial single-component molecular conductor with $\pi-$d multifrontier orbitals. In addition, (^{n}Bu$_4$N)$_2$[Cu(tmdt)$_2$] was synthesized, and its crystal structure was determined. Its Curie behavior ($\chi_{rt} = 1.2 \times 10^{-3}$ emu mol^{-1}; $C = 0.36$ emu·K mol^{-1}) indicates the existence of an isolated $S = 1/2$ spin on each dianionic molecule.

Introduction

Electron conduction is one of the most fundamental electronic functions of molecular solids. Since the discovery of the first organic superconductor,[1] the field of molecular conductors has become highly developed, and various types of molecular conductors have been reported, including rare systems such as field-induced organic superconductors[2] and organic thyristors.[3] However, many hurdles remain to further progress: One serious problem is the low phase transition temperature T_c. For example, the widely accepted T_c-record for an organic superconductor is still only 14 K,[4] and the ferromagnetic transition temperature of a magnetic organic metal is only around 10 K.[5] The conventional molecular conductor has a fatal weakness in that its inherent low-dimensionality tends to suppress T_c. In this respect,

*To whom correspondence should be addressed. E-mail: akoba@chs.nihon-u.ac.jp (A.K.), hayao@chs.nihon-u.ac.jp (H.K.).

(1) (a) Jerome, D.; Mazaud, A.; M. Ribault, M.; Bechgaard, K. *J. Phys., Lett*. **1980**, *41*, L95–L98. (b) Jerome, D. *Chem. Rev*. **2004**, *104*, 5565–5591.

(2) (a) Uji, S.; Shinagawa, H.; Terashima, T.; Yakabe, T.; Terai, Y.; Tokumoto, M.; Kobayashi, A.; Tanaka, H.; Kobayashi, H. *Nature* **2001**, *410*, 908–910. (b) Fujiwara, H.; Kobayashi, H.; Fujiwara, E.; Kobayashi, A. *J. Am. Chem. Soc*. **2002**, *124*, 6816–6817. (c) Kobayashi, H.; Cui, H.; Kobayashi, A. *Chem. Rev*. **2004**, *104*, 5265–5288.

(3) Sawano, F.; Terasaki, I.; Mori, H.; Mori, T.; Watanabe, M.; Ikeda, N.; Nogami, Y.; Noda, Y. *Nature* **2005**, *437*, 522–524.

(4) (a) Taniguchi, H.; Miyashita, M.; Uchiyama, K.; Satoh, K.; Mori, N.; Okamoto, H.; Miyagawa, K.; Kanoda, K.; Hedo, M.; Uwatoko, Y. *J. Phys. Soc. Jpn*. **2003**, *72*, 468–471.

(5) (a) Coronado, E.; Galán-Mascarós, J. R.; Gómez-García, C. J.; Laukhin, V. *Nature* **2000**, *408*, 447–449. (b) Coronado, E.; Day, P. *Chem. Rev*. **2004**, *104*, 5419–5448.

 Published on Web 06/14/2010

recently developed single-component molecular metals such as [M(tmdt)$_2$] (M = Ni, Pt, Au; tmdt = trimethylenetetrathiafulvalenedithiolate) are highly promising.[6,7] In fact, [Au(tmdt)$_2$] was found to undergo an antiferromagnetic transition at 110 K while retaining its metallic state.[8] It has been pointed out that the three-dimensionality of the electronic band structure of [M(tmdt)$_2$] is responsible for its extremely high T_c relative to the magnetic transition temperatures of conventional molecular conductors.[9,10] In addition, [M(tmdt)$_2$] has another attractive characteristic in that its electronic structure can be widely tuned by exchanging the central transition metal atom (M). In most molecular metals, the conduction bands are formed from only a single kind of π frontier orbital, which makes the electronic band structure of a molecular conductor very clear but somewhat monotonous. However, if the energy level of a d-like molecular orbital of M(tmdt)$_2$, which is constructed mainly from the d orbital of the central M atom and p orbitals of the surrounding S atoms of the ligands, are located near the Fermi level (ε_F) of the metal band formed primarily from π-like ligand orbitals, then non-trivial conductors such as molecular conductors with periodically arranged localized magnetic moments, molecular metals with π−d multibands, and even unprecedented molecular heavy electron systems might be realized. Considering that the energy level of the d orbital of Cu tends to be located near the energy level of the frontier orbitals of organic π molecules, we synthesized [Cu(tmdt)$_2$] to prepare a single-component molecular conductor with π−d multifrontier orbitals.

Experimental Section

General Methods. All the syntheses shown in Scheme 1 were performed under a strictly inert atmosphere using the Schlenk technique because the anionic states of the metal complexes are quite sensitive to oxygen. The tmdt ligand **3** was synthesized by a pseudo-Wittig reaction according to a procedure described in the literature.[11] Copper(II) chloride dihydrate ($Cu^{II}Cl_2\cdot 2H_2O$) was recrystallized with distilled water and dried in air. Tetrahydrofuran (THF) was freshly distilled under an argon atmosphere over sodium and benzophenone. Methanol (MeOH) was distilled under an argon atmosphere over magnesium metal activated with iodine. The supporting electrolyte tetra-*n*-butylammonium hexafluorophosphate ($^nBu_4N\cdot PF_6$) used in the electrocrystallization was recrystallized three times with ethylacetate and dried in vacuo. Acetonitrile (MeCN) was distilled under an argon atmosphere in the presence of calcium hydride. All other reagents were used without purification.

Scheme 1[a]

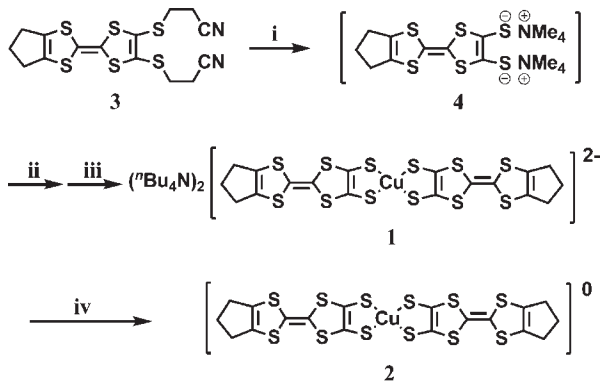

[a] Reagents and conditions: (i) 25-wt % $Me_4N\cdot OH$/MeOH (4 equiv), dry THF, room temperature, 30 min. (ii) $Cu^{II}Cl_2\cdot 2H_2O$/MeOH (0.5 equiv), −78 °C to room temperature, overnight. (iii) Cation exchange in $^nBu_4N\cdot PF_6$/MeCN solution. (iv) Electrochemical oxidation in $^nBu_4N\cdot PF_6$/MeCN solution.

Synthesis of ($^nBu_4N$)$_2$[Cu(tmdt)$_2$] (1). Ligand **3** (126 mg; 0.304 mmol) was hydrolyzed with a 25-wt % MeOH solution of tetramethylammonium hydroxide ($Me_4N\cdot OH$) (440 mg; 1.21 mmol) in dry THF (15.0 mL) at room temperature and under an argon atmosphere. The solution was stirred for 30 min, and a reddish-orange intermediate precipitate **4** was obtained as the reaction proceeded. After cooling to −78 °C in a dry ice/MeOH bath, a solution of $Cu^{II}Cl_2\cdot 2H_2O$ (25.6 mg; 0.150 mmol) in dry MeOH (5.0 mL) was added dropwise to the reaction mixture. Then the reaction mixture was warmed to room temperature overnight. The resulting microcrystals were collected by filtration and crystallized from a MeCN solution of $^nBu_4N\cdot PF_6$ at room temperature under an argon atmosphere to afford dark-orange crystals of **1**.

Electrochemical Synthesis of [Cu(tmdt)$_2$] (2). All the electrochemical oxidation was performed in a standard H-type cell without glass frits using two platinum electrodes under an argon atmosphere. Complex **1** (15.0−20.0 mg; 12.9−17.2 × 10^{-3} mmol) and $^nBu_4N\cdot PF_6$ (250.0 mg; 0.645 mmol) were dissolved in dry MeCN (40.0 mL) under an argon atmosphere. Electrochemical oxidation of this solution was performed with a constant current of 0.4 μA at room temperature. Air-stable black microcrystals of **2** grew on the anode within approximately 4 weeks.

Crystal Structure Determination of 1 and 2. Single crystals of **1** and **2** were analyzed at 293 K on a Rigaku Micro7HFM-VariMax Saturn 724R CCD system equipped with graphite monochromated Mo Kα radiation (λ = 0.71073 Å) and a confocal X-ray mirror. The crystal data and details of the crystal structure determination experiment are listed in Table 1. The crystals used for data collection were about 0.20 mm × 0.10 mm × 0.10 mm in size for **1** and 0.07 mm × 0.02 mm × 0.01 mm in size for **2**. The crystal structures were determined by direct methods (SIR92).[12] Anisotropic temperature factors were applied for the non-hydrogen atoms. The calculated positions of the hydrogen atoms were not refined but included in the final calculations. All the calculations were performed using the CrystalStructure crystallographic software package of the Molecular Structure Corp.[13]

(6) (a) Tanaka, H.; Okano, Y.; Kobayashi, H.; Suzuki, W.; Kobayashi, A. *Science* **2001**, *291*, 285–287. (b) Kobayashi, A.; Tanaka, H.; Kobayashi, H. *J. Mater. Chem.* **2001**, *11*, 2078–2088. (c) Kobayashi, A.; Fujiwara, E.; Kobayashi, H. *Chem. Rev.* **2004**, *104*, 5243–5264.

(7) In the paper, [M(L)$_2$] and M(L)$_2$ (L = ligand) are used to denote the crystal and the molecule of M(L)$_2$, respectively.

(8) (a) Suzuki, W.; Fujiwara, E.; Kobayashi, A.; Fujishiro, Y.; Nishibori, E.; Takata, M.; Sakata, M.; Fujirawa, H.; Kobayashi, H. *J. Am. Chem. Soc.* **2003**, *125*, 1486–1487. (b) Zhou, B.; Shimamura, M.; Fujiwara, E.; Kobayashi, A.; Higashi, T.; Nishibori, E.; Sakata, M.; Cui, H.; Takahashi, K.; Kobayashi, H. *J. Am. Chem. Soc.* **2006**, *128*, 3872–3873. (c) Ishibashi, S.; Tanaka, H.; Kohyama, M.; Tokumoto, M.; Kobayashi, A.; Kobayashi, H.; Terakura, K. *J. Phys. Soc. Jpn.* **2005**, *74*, 843–846.

(9) Hara, Y.; Miyagawa, K.; Kanoda, K.; Shimamura, M.; Zhou, B.; Kobayashi, A.; Kobayashi, H. *J. Phys. Soc. Jpn.* **2008**, *77*, 053706.

(10) Seo, H.; Ishibashi, S.; Okano, Y.; Kobayashi, H.; Kobayashi, A.; Fukuyama, H.; Terakura, K. *J. Phys. Soc. Jpn.* **2008**, *77*, 023714.

(11) (a) Binet, L.; Fabre, J. M.; Montginoul, C.; Simonsen, K. B.; Becher, J. *J. Chem. Soc., Perkin Trans. 1* **1996**, 783–788. (b) Binet, L.; Montginoul, C.; Fabre, J. M.; Ouahab, L.; Golhen, S.; Becher, J. *Synth. Met.* **1997**, *86*, 1825–1826. (c) Fujiwara, E.; Kobayashi, A.; Fujiwara, H.; Kobayashi, H. *Inorg. Chem.* **2004**, *43*, 1122–1129.

(12) *SIR92*: Altomare, A.; Burla, M. C.; Camalli, M.; Cascarano, M.; Giacovazzo, C.; Guagliardi, A.; Polidori, G. *J. Appl. Crystallogr.* **1994**, *27*, 435.

(13) *CrystalStructure 3.6.0; Crystal Structure Analysis Package*; Rigaku and Rigaku/MSC: The Woodlands, TX, 2000−2004.

Table 1. X-ray Crystallographic Data of the Copper Complexes **1** and **2**

	$(^nBu_4N)_2$ $[Cu(tmdt)_2]$	$[Cu(tmdt)_2]$
empirical formula	$C_{50}H_{84}CuN_2S_{12}$	$C_{18}H_{12}CuS_{12}$
formula weight	1161.49	676.56
crystal color	dark brown	black
crystal system	monoclinic	triclinic
lattice parameters		
a (Å)	15.620(5)	6.4598(8)
b	19.867(7)	7.3626(9)
c	20.005(7)	12.1205(13)
α (deg)	90.000	91.064(4)
β	104.265(5)	96.755(4)
γ	90.000	104.006(4)
V (Å^3)	6017(3)	554.8(1)
space group	$P2_1/c$ (No. 14)	$P\bar{1}$ (No. 2)
Z value	4	1
D_{calc} (g/cm^3)	1.282	2.025
μ(Mo Kα) (cm^{-1})	8.130	21.227
diffractometer	Rigaku Saturn CCD	Rigaku Saturn CCD
radiation	Mo Kα (λ = 0.71070 Å)	Mo Kα (λ = 0.71070 Å)
T (K)	293	293
no. of reflections measured		
total	64344	4212
unique	13681	2964
structure solution	direct methods (SIR92)	direct methods (SIR92)
no. observations ($I > 2\sigma$)	29334	2027
no. variables	671	149
residuals: R_1 ($I > 2\sigma$) [a]	0.0696	0.0678
residuals: wR_2 ($I > 2\sigma$) [b]	0.0875	0.0785
GOF indicator	1.138	1.214

[a] $R_1 = \sum||F_o| - |F_c||/\sum|F_o|$. [b] $wR_2 = [\sum w(F_o^2 - F_c^2)^2/\sum wF_o^2]^{1/2}$.

Magnetic Measurements of 1 and 2. Magnetic measurements of **1** (1.37 mg; 1.18×10^{-3} mmol) and **2** (7.67 mg; 1.13×10^{-2} mmol) were performed with a Quantum Design MPMS-7XL superconducting quantum interference device (SQUID) magnetometer. Samples were wrapped in a clean aluminum foil whose magnetic susceptibility was separately measured and subtracted. The static magnetic susceptibilities (χ) of **1** and **2** were measured in the temperature range from 2.0 to 300 K at an applied magnetic field of 0.5 T. And the static magnetic susceptibility of **2** was also measured in the temperature range from 2.0 to 30 K at applied magnetic fields of 0.3, 0.5, 0.75, 1.0, 1.5, 2.0, and 3.0 T. The diamagnetic contribution was calculated from Pascal's constants ($\chi^{dia} = -7.3 \times 10^{-4}$ emu·mol^{-1} and -3.1×10^{-4} emu·mol^{-1} for **1** and **2**, respectively).

Electron Spin Resonance (ESR) Measurements of 2. The ESR spectra of **2** (5.65 mg; 8.35×10^{-3} mmol) microcrystals were measured using a JEOL JES-FA200 ESR spectrometer and the low-temperature unit JEOL ES-CT470 in the temperature range of 4.6−291 K. Applied microwave power was 1.0 mW, and the modulation field was about 9.0 G.

Electrical Resistivity Measurements of 2. Four-probe resistivity measurements were performed on compressed pellets of polycrystalline samples of **2** in the temperature range 4−300 K using a Huso Electro Chemical System HECS 994C-1 multichannel four-terminal conductometer. Annealed gold wires (15 μm in diameter) bonded to the sample by gold paint were used as leads. The temperature dependence of resistivity was also examined up to 15 kbar by using a conventional clump-type high-pressure cell and samples coated with epoxy resin. A calibrated Cerenox thermometer was used over the entire temperature range.

Molecular Orbital Calculations of 1 and 2. Spin-polarized calculations were performed at the density functional theory (DFT) level with DMol^3 codes[14,15] using the Generalized Gradient Approximation (GGA) and the exchange and correlation functionals of Becke and Lee, Yang, and Parr (BLYP), respectively. Double numerical basis sets plus polarization functions (DNP) were used in the calculations, and a global orbital cutoff of 4.4 Å was used. The density convergence criterion for the self-consistent field optimization energy was set to 10^{-6} hartree.

Results and Discussion

Structural Characterization of 1. Figures 1a and 1b show the molecular structure of the dianion complex $[Cu(tmdt)_2]^{2-}$ in **1**, and Figures 1c and 1d show the packing diagram viewed along different axes. There is one crystallographically independent $[Cu(tmdt)_2]^{2-}$ anion and two $^nBu_4N^+$ cations in the unit cell. The coordination geometry of $[Cu(tmdt)_2]^{2-}$ is fairly distorted from planar with Cu−S distances of 2.279−2.282 Å in one ligand and 2.286−2.292 Å in another ligand. The dihedral angle between the two least-squares planes of CuS_2C_2 five-membered rings is 29.4° (Figure 1b), which is slightly smaller than that for the similar copper dithiolate complexes such as $[Cu(dmdt)_2]^{2-}$ (33.5°) (dmdt = dimethyltetrathiafulvalenedithiolate)[16] and $[Cu(ptdt)_2]^{2-}$ (57.3°) (ptdt = propylenedithiotetrathiafulvalenedithiolate).[17] Furthermore, the angle formed from the two centroids of the S−Cu−S planes and the central copper atom is 174.6°, indicating the coordination geometry of CuS_4 is also faintly curved. The geometry of the two tmdt ligands around the copper atom is unsymmetrical: one ligand is somewhat bent at the positions of the sulfur atoms of the tetrathiafulvalene (TTF) part with a dihedral angle of 6.8°, and another one is noticeably bent with a dihedral angle of 18.6°. However, the C=C distances are 1.310−1.341 Å, and there is no significant difference in both ligands.

As shown in Figures 1c and 1d, the $[Cu(tmdt)_2]^{2-}$ anions are arranged such that their molecular long axes are parallel to each other and the c-axis and the molecular planes are stacked along the a-axis. These layers are separated by the bulky tetra-n-butylammonium cations along the b-axis. The shortest intermolecular S···S distance in the crystal is 3.958 Å. The shortest intermolecular Cu···Cu distance of 7.823 Å is observed between the $[Cu(tmdt)_2]^{2-}$ anions arranged along the a-axis, as shown in Figure 1d.

Structural Characterization of 2. The X-ray powder diffraction experiment revealed that **2** belonged to the triclinic system and was isostructural with other $[M(tmdt)_2]$ conductors (M = Ni, Pt, Au).[6,8,18] The powder diffraction data of **2** is shown in the Supporting Information. Recently single-crystal structure determination could be done with microsingle crystals (maximum size of about 70 μm). The geometry around the Cu atom was found to

(14) (a) Delley, B. *J. Chem. Phys.* **1990**, *92*, 508–517. (b) Delley, B. *J. Chem. Phys.* **2000**, *113*, 7756–7764; DMol^3 is available as part of Material Studio.
(15) Perdew, J. P.; Burke, K.; Ernzerhof, M. *Phys. Rev. Lett.* **1996**, *77*, 3865–3868.
(16) Tanaka, H.; Kobayashi, H.; Kobayashi, A. *J. Am. Chem. Soc.* **2002**, *124*, 10002–10003.
(17) Kumasaki, M.; Tanaka, H.; Kobayashi, A. *J. Mater. Chem.* **1998**, *8*, 301–307.
(18) Zhou, B.; Kobayashi, A.; Okano, Y.; Nakashima, T.; Aoyagi, S.; Nishibori, E.; Sakata, M.; Tokumoto, M.; Kobayashi, H. *Adv. Mater.* **2009**, *21*, 3596–3600.

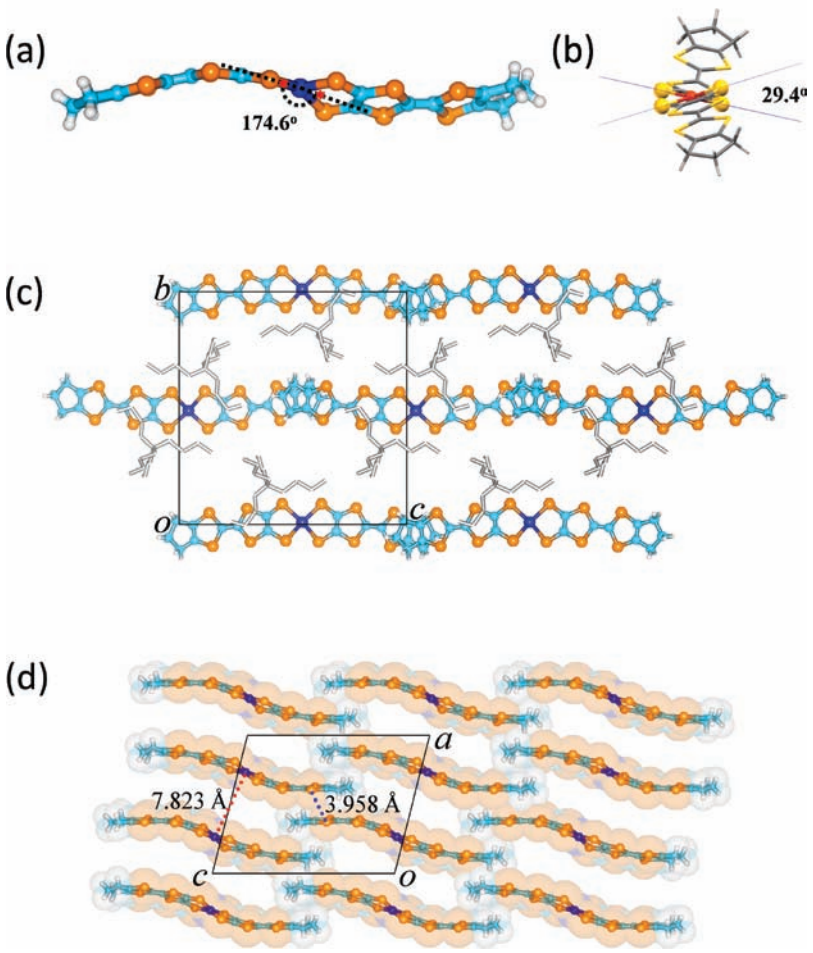

Figure 1. (a) Molecular structure of dianion copper complex in **1**. (b) The dihedral angle of two S−Cu−S planes connected to the central Cu atom. (c) The crystal structure of **1** viewed along the *a* axis. (d) The crystal structure of **1** viewed along the *b* axis. The shortest intermolecular S···S distance in the crystal is 3.958 Å The shortest intermolecular Cu···Cu distance of 7.823 Å is observed between the $[Cu(tmdt)_2]^{2-}$ anions arranged along the *a*-axis.

be square-planar, and the two extended TTF ligands are essentially coplanar. The neutral complex **2** shows Cu−S distances of 2.284(2) Å. On the basis of the relation between the metal−ligand bond length and the bond valence sum (or the oxidation of the metal ion) proposed by Brown,[19] the oxidation state of the Cu atom in $Cu(tmdt)_2$ was estimated to be +2.0. However, the C=C distance in the TTF ring is 1.363−1.380 Å, which is longer than that of the dianion complex. Thus, electrochemical oxidization was mainly carried out from the extended-TTF ligands of the dianion complex to those of the neutral one.

As shown in Figure 2a, the $Cu(tmdt)_2$ molecule assumes a planar structure, unlike the tetrahedral conformation of the $Cu(dmdt)_2$ molecule with similar extended-TTF type ligands.[16] According to Ishibashi,[20] the structure of an isolated $M(tmdt)_2$ (M = Ni, Au) molecule is most stable when the molecule has a planar structure. By contrast, the tetrahedral conformation is more stable in $Cu(tmdt)_2$, although the energy difference is not large (~0.1 eV). It is probable that the observed planar structure of $Cu(tmdt)_2$ is due to the small energy difference between the planar and tetrahedral conformations and the superior molecular packing in the planar structure. As shown in Figure 2b, many intermolecular short S···S contacts are present along the *a* axis. The shortest S···S distance (3.380 Å) is significantly shorter than the corresponding van der Waals distance (3.70 Å) but is comparable to the shortest S···S distances in other $M(tmdt)_2$ molecules: 3.391 Å (M = Ni), 3.344 Å (Au), and 3.362 Å (Pt). The shortest intermolecular S···S distances along the *b* and *c* axes are 3.660 Å (S4(x,y,z)···S5(1−x,1−y,1−z)) and 3.740 Å (S2(x,y,z)···S6(−x,−y,1−z)), respectively.

Electronic Structure of 2. As mentioned previously, the electronic structure of $M(tmdt)_2$ can be changed systematically by exchanging the central metal atom (M). According to ab initio calculations performed by Ishibashi et al.,[20] the energy level of d-like orbitals of the $Cu(dmdt)_2$ molecule is near those of π-like frontier orbitals. Our GGA-DFT calculations on $M(tmdt)_2$ (M = Pt, Ni, Au, Cu) with the DMol^3 code[14,15] showed that, as reported previously,[6] the lowest unoccupied molecular orbital (LUMO) of $Ni(tmdt)_2$ and the singly occupied molecular orbital (SOMO) of $Au(tmdt)_2$ are essentially the same, composed of an antisymmetric combination of the left- and right-ligand π orbitals and a small contribution of the d orbital

(19) (a) Brown, I. D.; Altermatt, D. *Acta Crystallogr.* **1985**, *B41*, 244–247. (b) Liu, W. T.; Thorp, H. H. *Inorg. Chem.* **1993**, *32*, 4102–4105. (c) Shields, G. P.; Raithby, P. R.; Allen, F. H.; Motherwell, W. D. S. *Acta Crystallogr.* **2000**, *B56*, 455–465.

(20) Ishibashi, S.; Terakura, K.; Kobayashi, A. *J. Phys. Soc. Jpn.* **2008**, *77*, 024702.

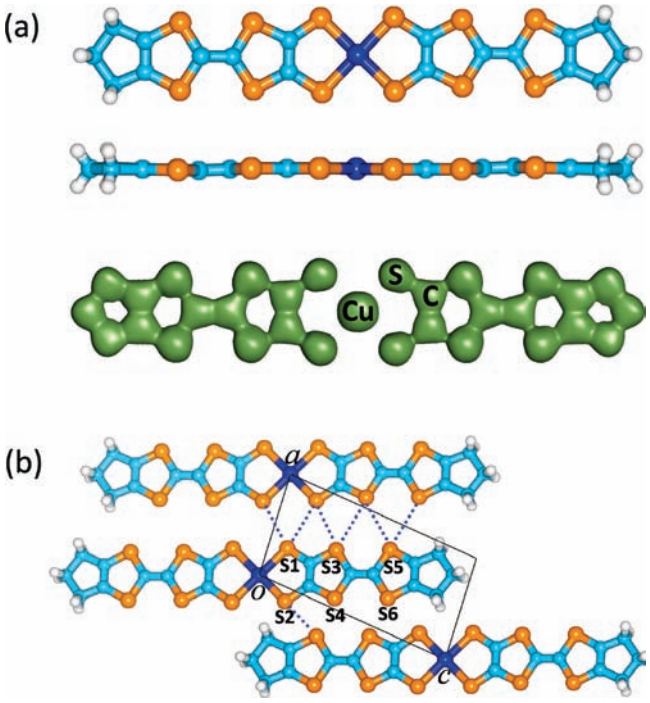

Figure 2. (a) Molecular structure of $Cu(tmdt)_2$ and the electron density distribution of $Cu(tmdt)_2$ determined by MEM and Rietveld analyses as equicontour surface of 0.4 e^{-3}. (b) The crystal structure of **2** viewed along the *b* axis. There are many short S···S contacts between the adjacent molecules. The shortest S···S contact (3.380 Å) is that along the *a* axis, which is fairly shorter than the corresponding van der Waals distance (3.70 Å) and is almost equal to the shortest contact in $[Ni(tmdt)_2]$ (3.391 Å). The shortest intermolecular S···S distances along the *b* and *c* directions are 3.660 Å (S4(x,y,z)···S5($1-x$, $-y$, $1-z$)) and 3.740 Å (S2(x,y,z)···S6($-x$, $-y$,$1-z$)), respectively, where S*i*(x,y,z) is the *i*-th S atom of the molecule on (0,0,0).

of the central transition metal atom. We refer to these orbitals as asym-Lπ(d) (Figure 3a).[21] Similarly, the highest occupied molecular orbital (HOMO) of $Ni(tmdt)_2$ and the SOMO-1 of $Au(tmdt)_2$ are composed of a symmetric combination of the π orbitals of the left and right ligands, (sym-Lπ). The d-like orbital has been named pdσ(-) by Ishibashi et al.[20] The calculated energy differences (Δ) between the pdσ(-) and asym-Lπ(d) states of $M(tmdt)_2$ were 0.7 and 1.2 eV for M = Ni and Pt, respectively, consistent with the values obtained in the previous report by Ishibashi (Δ(Ni) $\sim$ 0.54 eV).[20] Ishibashi also pointed out that Δ becomes very small in $Au(tmdt)_2$ (Δ(Au) $\sim$ 0.2 eV),[20] which is also consistent with the present results (Δ(Au) $\sim$ 0.17 eV).

We performed spin-polarized calculations on $Cu(tmdt)_2$. As shown in Figure 3a, the energy of the α-spin state of pdσ(-) and those of the α- and β-sym-Lπ states are almost degenerate, which is the most important feature of the electronic structure of $Cu(tmdt)_2$. In contrast to the nearly spin-independent sym-Lπ and asym-Lπ(d) states, the α- and β-pdσ(-) states are separated by approximately 0.54 eV, suggesting a tendency for the appearance of a magnetic moment. Since the energy separation between the asym-Lπ(d) and sym-Lπ states is estimated to be 0.26 eV, the vacant asym-Lπ(d) state and the doubly occupied sym-Lπ state are thought to form metal bands similar to those of $Ni(tmdt)_2$ when the singly occupied pdσ(-) state does not exist.[6,8c,22,23] However, since the α-pdσ(-) state exists just around ε_F of the virtual metal band formed from the asym-Lπ(d) and sym-Lπ states, the electronic properties can be changed dramatically by $\pi-$d interactions (or pdσ(-)$-$sym-Lπ and pdσ(-)$-$asym-Lπ(d) interactions).

Spin-polarized calculations on the $[Cu(tmdt)_2]^{2-}$ dianion were also performed. The energy diagram in Figure 3b indicates the mixing of the energies of the α-spin state of pdσ(-) with those of the α- and β-sym-Lπ states and α- and β-asym-Lπ(d) states, probably because both ligands have a slightly bent structure. The β-pdσ(-) state is 0.46 eV above the β-asym-Lπ(d) state. The spin density distribution of $[Cu(tmdt)_2]^{2-}$ shown in Figure 3c suggests that the calculated spin density distribution is consistent with the magnetic susceptibility measurement showing that Cu^{2+} spin ($S = 1/2$) is almost localized. Figure 3c also shows that the spin density distribution of $Cu(tmdt)_2$ is similar to that of the dianion $[Cu(tmdt)_2]^{2-}$ with spin density localized on the central Cu atom.

Magnetic Properties of 1 and 2. The magnetic susceptibilities ($\chi(T)$) of polycrystals of **1** and **2** were measured by a SQUID magnetometer. Curie behavior was observed for the dianion complex **1** ($\chi_{rt} = 1.2 \times 10^{-3}$ emu/mol, $C = 0.36$ emu·K/mol), indicating the existence of an isolated $S = 1/2$ spin on each molecule. The temperature dependence of the susceptibility of the neutral complex **2** also clearly showed the presence of a localized moment ($S = 1/2$) on each $Cu(tmdt)_2$ molecule (Figure 4a). However, the temperature dependence of the magnetic susceptibility of **2** indicated behavior consistent with an antiferromagnetic Heisenberg chain. At 20 K $< T <$ 250 K, $\chi(T)$ is well fitted by the following equation:[24] $\chi(T) = \rho(Ng^2\beta^2/kT)(0.25 + 0.074975x + 0.075235x^2)/(1.0 + 0.9931x + 0.172135x^2 + 0.757825x^3) + (1 - \rho)(0.375/T)$, where $x = |J|/kT$, $\rho = 0.975$, $|J| = 117.4\ cm^{-1}$, and $g = 2.048$. At around 13 K, a susceptibility anomaly was observed. Since the lower-quality sample showed a larger increase in the susceptibility at low temperature, the increase in χ at low temperature (or the second term of $\chi(T)$) is considered to be due to paramagnetic impurities. Above 250 K, the observed temperature dependence of susceptibility shows a significant deviation from the calculated $\chi(T)$ curve, suggesting a contribution from π conduction electrons. Below 13 K, the susceptibility showed field dependence. Because the susceptibility of paramagnetic impurities tends to mask the intrinsic magnetic behavior at low temperature, the temperature dependences of $[\chi(H) - \chi(3T)]$ were examined to eliminate the impurity effect and to extract the magnetic field dependence of the susceptibilities (Figure 4b). $[\chi(H) - \chi(3T)]$ was negative at $H < 1.5$ T but became approximately zero

(21) Zhou, B.; Kobayashi, A.; Okano, Y.; Cui., H.; Graf, D.; Brooks, J. S.; Nakashima, T.; Aoyagi, S.; Nishibori, E.; Sakata, M.; Kobayashi, H. *Inorg. Chem.* **2009**, *48*, 10151–10157.

(22) Rovira, C.; Novoa, J. J.; Mozos, J. L.; Ordejón, P.; Canadell, E. *Phys. Rev. B* **2002**, *65*, 081104.

(23) Tanaka, H.; Tokumoto, M.; Ishibashi, S.; Graf, D.; Choi, E. S.; Brooks, J. S.; Yasuzuka, S.; Okano, Y.; Kobayashi, H.; Kobayashi, A. *J. Am. Chem. Soc.* **2004**, *126*, 10518–10519.

(24) (a) Estes, W. E.; Gavel, D. P.; Hatfield, W. E.; Hodgson, D. J. *Inorg. Chem.* **1978**, *17*, 1415–1421. (b) Girerd, J. J.; Kahn, O.; Verdaguer, M. *Inorg. Chem.* **1980**, *19*, 274–276.

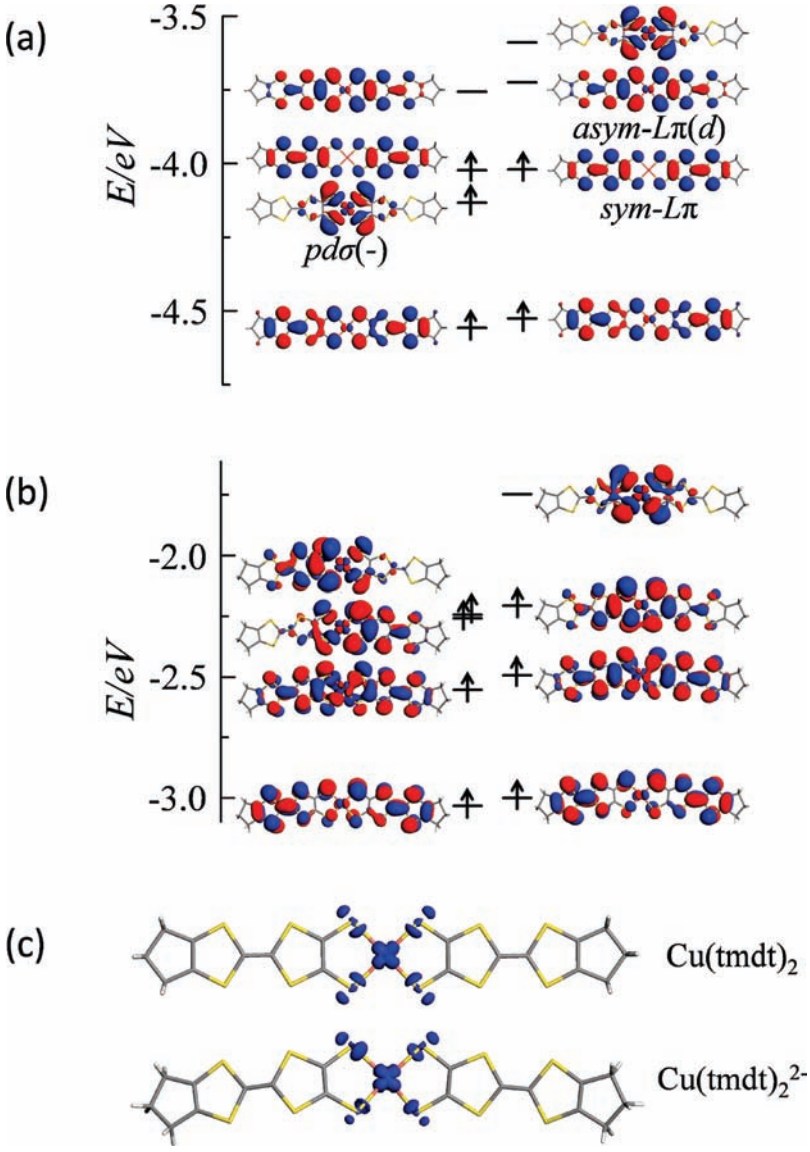

Figure 3. (a) Spin polarized molecular orbitals and the energy levels of $Cu(tmdt)_2$ molecule. (b) Spin polarized molecular orbitals and the energy levels of $[Cu(tmdt)_2]^{2-}$ anion. (c) Spin density distributions of $Cu(tmdt)_2$ molecule and $[Cu(tmdt)_2]^{2-}$ anion using isosurfaces of 0.05 au.

at $H = 2$ T. These results clearly indicate an antiferromagnetic transition at around 13 K. The spin-flop field appears to be close to 1 T. The magnetic behavior of **2** is reminiscent of the electromagnetic properties of the well-known prototypal $\pi-d$ magnetic organic conductor (R_1, R_2-DCNQI)$_2$Cu (R_1, R_2 = CH_3, Cl; CH_3, Br; Br, Br; Cl, Cl; and DCNQI = dicyanoquinonediimine), where π-acceptor molecules and tetrahedrally coordinated copper counter-cations form a unique $\pi-d$ system.[25,26] However, it was found that in (R_1,R_2-DCNQI)$_2$Cu, the coexistence of conduction electrons and magnetic moments cannot be achieved. The Cu^{2+} moments appear only in the insulating phase and undergo antiferromagnetic ordering at low temperatures (~10 K). In contrast, the localized magnetic moments and conduction electrons seem to coexist in $[Cu(tmdt)_2]$, as shown below.

Since the spins are considered to be distributed mainly in the pdσ(-) orbitals, the anisotropy of the antiferromagnetic interaction can be roughly estimated from the anisotropy of the intermolecular overlap integrals (S) of pdσ(-) ($J \propto S^2$). Considering that this orbital is a σ-type orbital and has a large amplitude only in the central part of the molecule ($[CuS_4]$), the J-value along the a axis will be much larger than those along the b and c axes (see the inset of Figure 4a). This is consistent with the one-dimensional magnetic behavior of $[Cu(tmdt)_2]$. The overlap integrals are shown in reference 27.

(25) (a) Aumüller, A.; Erk, P.; Klebe, G.; Hünig, S.; von Schütz, J. U.; Werner, H.-P. *Angew. Chem., Int. Ed. Engl.* **1986**, *25*, 740–741. (b) Hünig, S.; Herberth, E. *Chem. Rev.* **2004**, *104*, 5535–5563.

(26) (a) Kobayashi, A.; Kato, R.; Kobayashi, H.; Mori, T.; Inokuchi, H. *Solid State Commun.* **1987**, *64*, 45–51. (b) Kato, R.; Kobayashi, A.; Kobayashi, H. *J. Am. Chem. Soc.* **1989**, *111*, 5224–5232. (c) Kobayashi, H.; Miyamoto, A.; Kato, R.; Sasaki, F.; Kobayashi, A.; Yamakita, Y.; Furukawa, Y.; Tasumi, M.; Watanabe, T. *Phys. Rev. B* **1993**, *47*, 3500–3516. (d) Uji, S.; Terashima, T.; Aoki, H.; Brooks, J. S.; Kato, R.; Sawa, H.; Aonuma, S.; Tamura, M.; Kinoshita, M. *Phys. Rev. B* **1994**, *50*, 15597–15601. (e) Kato, R. *Bull. Chem. Soc. Jpn.* **2000**, *73*, 515–534.

(27) The intermolecular overlap integrals (S) of pdσ(-) orbitals obtained by the extended Hückel calculations were 0.23×10^{-3}, $0.02 \times 10-3$, and $0.01 \times 10-3$ along the a, c, and b directions, respectively.

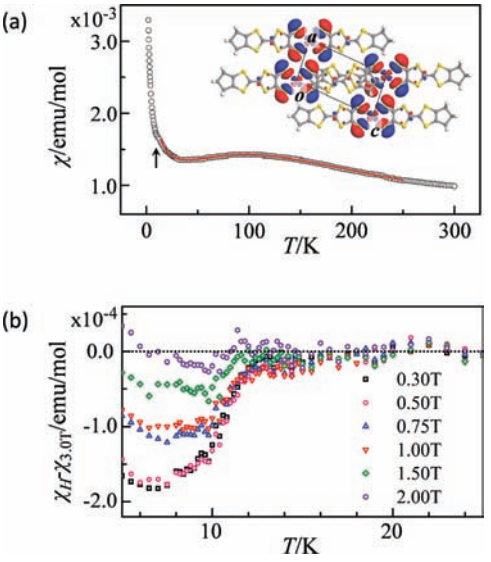

Figure 4. (a) Temperature dependence of magnetic susceptibility for **2**. The red line is a fitting curve based on an antiferromagnetic Heisenberg chain model (20 K $< T <$ 250 K). The inset shows the schematic image of pdσ~pdσ overlaps between the neighboring molecules along the *a* axis. (b) The low-temperature behavior of the magnetic field dependence of susceptibility.

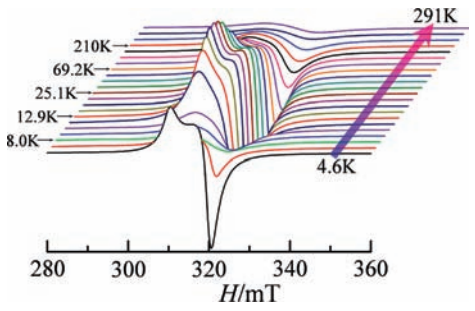

Figure 5. Temperature dependence of ESR signals of **2**.

Electron Spin Resonance Study of 2. The ESR spectra were measured at 4.6−291 K. The *g* values were estimated to be 2.078 and 2.024 at 18−100 K, respectively (Figure 5). The intensity showed a sudden drop, and the response profile changed drastically at around 13 K. This is consistent with the magnetic transition observed using SQUID measurements. However, the ESR behavior of **2** became unclear below 7 K, probably because of signals from paramagnetic impurities.

Electrical Properties of 2 at Ambient and High Pressure. Four-probe resistivity measurements were performed on compressed pellets of microcrystals of **2** (Figure 6). We observed fairly large room-temperature conductivity ($\sigma_{RT} \sim 7$ S·cm^{-1}), comparable to the conductivities of polycrystalline samples of conventional organic metals but smaller than those of polycrystalline samples of isostructural metallic [M(tmdt)$_2$] systems ($\sigma_{RT} = 200$ S·cm^{-1} (M = Ni),[6b] 350 S·cm^{-1} (M = Pt),[18] and 50 S·cm^{-1} (M = Au)[8b]). The temperature dependence of resistivity showed weakly semiconductive behavior with apparent activation energies of approximately 0.054 eV (150−250 K) at ambient pressure. The activation energy of resistivity measured by the powder sample at 15 kbar is almost half of that at 1 bar. [M(tmdt)$_2$] (M = Ni, Pt) without a single

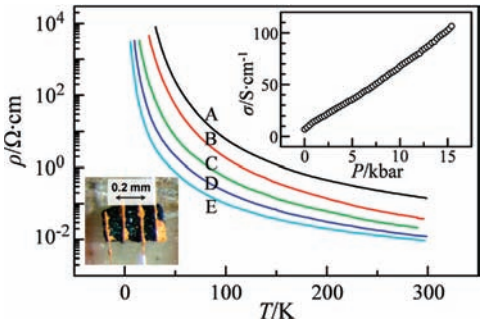

Figure 6. Temperature dependence of resistivities measured using compressed pellets of microcrystals of **2** (A, 1 bar; B, 3 kbar; C, 7 kbar; D, 11 kbar; E, 15 kbar). The inset shows a photograph of the compressed pellet sample and the pressure dependence of room-temperature conductivity.

occupied pdσ(-) orbital shows stable metallic properties. As expected, however, the presence of the pdσ(-) frontier orbital drastically changes the electromagnetic properties of [M(tmdt)$_2$] (M = Cu).

We also performed high-pressure resistivity measurements on samples coated with epoxy resin with four gold leads. As shown in the inset of Figure 6, the room-temperature conductivity increased almost linearly with pressure, reaching 110 S·cm^{-1} at 15 kbar. Unexpectedly, the temperature dependence of resistivity was almost unchanged despite the strongly enhanced conductivity at high pressure. Although the observed temperature dependence of resistivity for the compressed pellet showed non-metallic behavior, **2** can be essentially considered to be metallic at high pressures because such high conductivities have never been achieved in powder samples of non-metallic molecular conductors. At high pressures, the system will exhibit unique electronic properties. If the localized magnetic moments survive at high pressures, the system would become an unprecedented molecular conductor with periodically arranged, localized magnetic moments in which two types of frontier orbitals play essential roles. One is the σ-type frontier orbital with localized spins, and the other is the π-type frontier orbital responsible for metallic conduction. [Au(tmdt)$_2$] has been reported to be a single-component antiferromagnetic molecular metal;[8] however, the π-like orbitals (sym-Lπ, asym-Lπ(d)) are mainly responsible for both its electric and its magnetic properties. If the pdσ(-) orbitals tend to form a conduction band at high pressures, the system will become a molecular conductor with multiconduction bands having different characteristics. If this is the case, then the process by which localized moments disappear under high pressure will be of special interest, where a magnetic state with large spin susceptibility will change into a metallic state with small susceptibility. Such a situation, in which new electromagnetic properties may be expected, has never been realized in hitherto reported molecular conductors.

Conclusion

In conclusion, [Cu(tmdt)$_2$] is a new type of magnetic molecular conductor. At ambient pressure, the system behaves as an unprecedented, conducting, one-dimensional antiferromagnetic Heisenberg system that exhibits magnetic ordering at 13 K. At 15 kbar, it shows very high room-temperature

conductivity (110 $S \cdot cm^{-1}$) even in the form of a compressed pellet. This strongly suggests the metallic nature of [Cu(tmdt)$_2$] at high pressure. In the well-known prototypal $\pi-$d molecular conductor (R_1,R_2-DCNQI)$_2$Cu consisting of π-acceptor molecules and copper cations, the localized magnetic moments (Cu^{2+}) appear only in the insulating phase. Furthermore, in the previously reported single-component antiferromagnetic molecular metal [Au(tmdt)$_2$], the electromagnetic properties are mainly determined by π-like frontier molecular orbitals. However, [Cu(tmdt)$_2$] is an unprecedented single-component *multifrontier* $\pi-$d *system*. The introduction of a dσ-type frontier orbital around the Fermi level of the π-like metal band is expected to lead to the emergence of a new frontier for molecular conductors.

Acknowledgment. This study was financially supported by a Grant-in-Aid for Scientific Research (B) (No. 20350069), Grant-in-Aid for Young Scientists (B) (No. 21750153) and Innovative Areas (20110003) of Ministry of Education, Culture, Sports, Science and Technology of Japan. The study was also supported by the "Strategic Research Base Development" Program for Private Universities subsidized by MEXT (2009) (S0901022). The synchrotron radiation experiments were performed at the BL02B2 beamline of the SPring-8 facility with the approval of the Japan Synchrotron Radiation Research Institute (JASRI). We thank Prof. M. Tamura for the helpful discussions on the temperature dependence of magnetic susceptibility and Dr. Y. Nakai (JEOL) for the ESR measurements.

Supporting Information Available: The synchrotron radiation X-ray powder diffraction patterns of [M(tmdt)$_2$] (M = Ni, Au, Pt, Cu) are given in Figure S1 and the X-ray crystallographic files in CIF format for **1** and **2** (**single crystal**). This material is available free of charge via the Internet at http://pubs.acs.org.